Characterization of a Hall-Effect Radial Plasma Source

IEPC-2009-241
Presented at the 31st International Electric Propulsion Conference,
University of Michigan • Ann Arbor, Michigan • USA
September 20 – 24, 2009

Robert L. Washeleski[1], Jason M. Makela[2], and Lyon B. King[3]
Michigan Technological University, Houghton, MI, 49931, USA

A new Hall-effect radial plasma source (RPS) intended to simulate the plasma properties of a Hall-effect thruster (HET) was operated at a variety of conditions and the plasma near the channel exit was characterized using an electrostatic double probe. Electron temperature was found to range from 1 to 5 eV and electron density was found to range from 3 x 10^{15} m^{-3} to 6 x 10^{17} m^{-3}. These plasma conditions are similar to those found in the near-field plume of a HET. The RPS is intended to be a first step towards performing laser Thomson scattering (LTS) in the channel of an actual HET, with the main advantage of the RPS being simpler beam access for validation of the diagnostic. In addition to plume studies, the effects of mass flow rate, discharge current, and magnet current on operation of the RPS were determined. It was found that increasing the mass flow rate had no effect on electron density. Increasing the mass flow rate caused a decrease in electron temperature, presumably due to an increase in electron-neutral collisions. As discharge current was increased the electron temperature remained unchanged, while the density increased. Increasing the magnet current caused an increase in both density and electron temperature.

Nomenclature

A_p	=	probe area (m^2)
e	=	elementary charge (C)
I	=	probe current (A)
I_+	=	ion saturation current (A)
k	=	Boltzmann's constant (J/K)
m_i	=	ion mass (kg)
n_e	=	electron number density (m^{-3})
T_e	=	electron temperature (Kelvin)
V	=	probe voltage (V)

I. Introduction

THOMSON scattering is a laser diagnostic technique where a pulse or series of pulses from a laser are sent into a plasma and the spectra scattered from free electrons in the plasma are recorded. Using this technique, properties such as electron temperature and density can be determined in a non-invasive way from the intensity and shape of the measured spectra[1]. Specifically, the electron energy distribution can be directly measured in one dimension, and the three-dimensional energy distribution function can be calculated using a simple inversion procedure[2]. The electron properties are very important for nearly all plasmas, and this is especially true for space propulsion devices such as Hall-Effect thrusters (HETs). Electron dynamics in the discharge channel of a HET are critical to the performance and operation of the thruster, but taking accurate measurements in the channel is difficult for a number of reasons, including difficulty of access, excessive probe heating, and disruption of the plasma by conventional electrostatic probes.

[1] Ph.D Candidate, Mechanical Engineering-Engineering Mechanics, rlwashel@mtu.edu
[2] Ph.D Candidate, Mechanical Engineering-Engineering Mechanics, jmakela@mtu.edu
[3] Associate Professor, Mechanical Engineering-Engineering Mechanics, lbking@mtu.edu

The ISP Lab at Michigan Technological University is developing a laser Thomson Scattering (LTS) diagnostic with the goal of extending LTS to cathode and space propulsion plasmas, with an eventual goal of applying LTS to an actual HET. This requires an electron density detection limit on the order of 10^{16} m^{-3} and the ability to detect electron energies on the order of 1 eV, which is near the limit of current LTS diagnostics. To achieve these limits, baffles, beam dumps, and viewing dumps need to be carefully positioned to minimize stray light and maximize the very weak scattered signal. Thomson scattering is non-invasive to the plasma, but requires a path through the plasma that is being probed. The eventual goal of the MTU program is to modify a HET with optical access to accommodate the probe beam, allowing non-intrusive direct interrogation of the interior plasma using LTS. However, because thruster modifications will not be trivial researchers have identified an intermediate step that will allow validation of the LTS apparatus and technique in a plasma similar to that found within a HET. For ease of beam access and validation of the LTS system, a radially accelerated plasma source has been developed to simulate the properties of a HET discharge.

The objective of this study was to characterize the plasma density and temperature within the near-field plume of this new device, called the Hall-effect Radial Plasma Source (RPS). Various operating conditions were explored and the plasma near the device was mapped using electrostatic double probe measurements that can be compared to HET plasma conditions. The goal is to eventually confirm the probe measurements with the laser Thomson scattering technique, and then extend the laser diagnostic into the channel where the electrostatic probe data is difficult to obtain.

II. Experimental Apparatus and Methods

A. Vacuum Facility and Mass Flow Control

The experiment was run in Michigan Tech's Xenon Vacuum Test Facility, which is a 2-m-diameter vacuum chamber with a length of 4 m. Vacuum is maintained by two 48-inch cryogenic pumps with a combined pumping speed of 120,000 L/s (nitrogen) and a base pressure of approximately 2×10^{-6} Torr. The flow of krypton to the anode and cathode was controlled by two MKS 1479a mass flow controllers. Accuracy of the mass flow controllers is 1% of full scale, with a 200 sccm controller used for the anode and a 20 sccm controller used for the cathode. Tank pressure was measured by an ion gauge mounted to a flange on top of the vacuum chamber.

B. Hall-Effect Radial Plasma Source

The RPS is an axisymmetric device with radial electric field and axial magnetic field. This results in a Hall current about the axis of symmetry of the RPS and an ion "beam" that is exhausted radially outward from the entire circumference, providing zero net thrust. The electric field is created by a ring-like anode, which diffuses the gas that is fed into the end of the RPS. An internal coil with iron poles supplies the axial magnetic field. The discharge channel is 9.5 mm wide and 22 mm deep with boron nitride walls, which results in a channel cross-section that is similar to a HET in both field arrangement and physical proportion. The outer diameter of the RPS is 125 mm. A schematic can be seen in Figure 1.

Similar to a HET, the internal discharge chamber of the RPS has elevated temperatures and densities such that internal direct probe diagnostics are problematic. For initial experiments reported in this paper electrostatic probes only sampled plasma outside of the channel to avoid heating, ablation, and disruption of the plasma discharge that would occur if the probes were inserted within the channel. Future LTS measurements can be validated for the lower electron temperatures and densities found outside the channel, and then extended to the harsher environment of the channel itself. The open geometry of the channel allows a laser beam to be passed through the plasma and into a beam dump while allowing the collection optics to focus on a scattering volume that is inside the channel, but against the background of a viewing dump if care is taken in alignment.

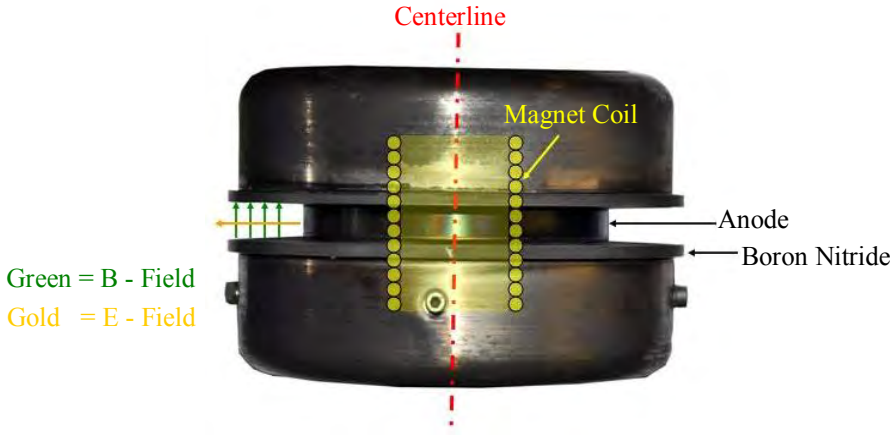

Figure 1. RPS schematic. Overlay graphic indicates internal arrangement of magnetic field coil.

C. Cathode

The cathode used was a laboratory cathode with a LaB_6 emitter fabricated in the ISP Lab. The body is made of titanium and measures approximately 25 mm in diameter by 100 mm long. The cathode orifice is 4 mm in diameter. All tests reported here utilized krypton as a discharge gas through both the cathode and the RPS anode. A tungsten keeper electrode is placed approximately 3.5 mm from the cathode face. During this experiment the cathode was operated at a mass flow rate 7 sccm while determining the operating characteristics, and 15 sccm during the probe measurements. The cathode was placed approximately 40 mm vertically above the end of the channel and 40 mm away from the center of the channel. A picture of the RPS and cathode in operation can be seen in Figure 2.

Figure 2. RPS operating on krypton.

D. Probes

The electrostatic probe consisted of two tungsten wires 0.05" in diameter inside an alumina sheath. The protruding length of the wires is 3.8 mm. The probe was mounted on a 3-axis motion table, which allows mapping of the plasma generated by the RPS for comparison with future LTS measurements. The probes were driven with a programmable source meter controlled by an automated measurement program. The voltage between the probe tips

was swept from -30 to 30 V in 0.06 V steps, with a measurement time of 16 msec at each voltage. Five sweeps were recorded at each measurement location, with the actual voltage and collected current recorded. Measurement locations formed a rectangular grid 16 mm by 25 mm with 4 mm spacing along the r-axis, and 5 mm spacing along the z-axis. The rectangular grid's edge closest to the RPS was 10 mm from the end of the channel. Sweeps were performed in pseudo-random order within the measurement grid. A schematic of the test setup can be seen in Figure 3 (roughly to scale).

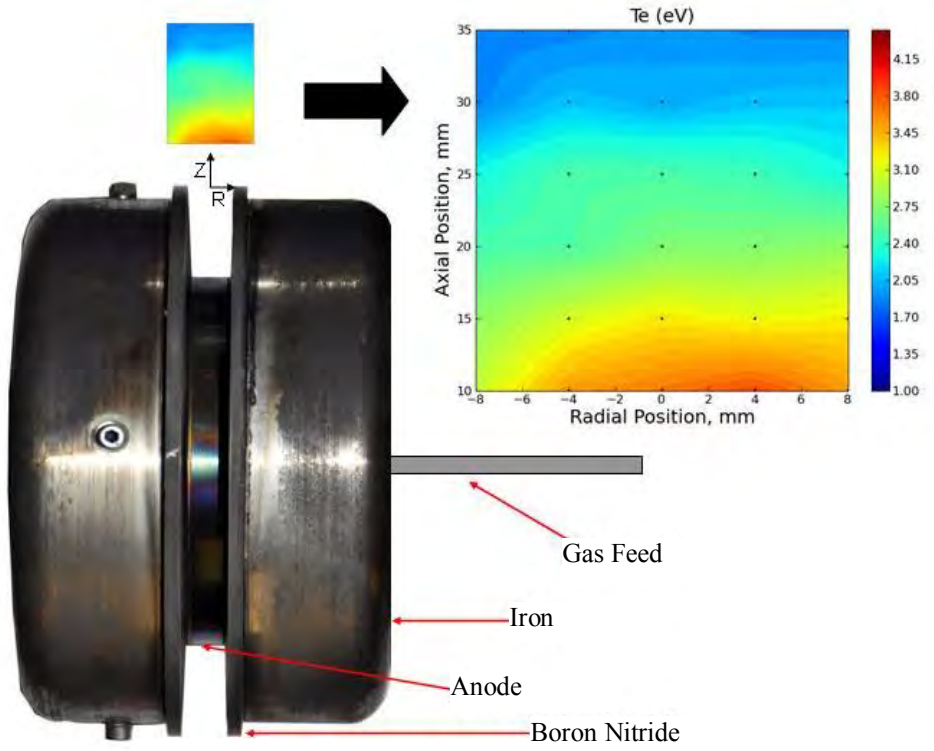

Figure 3. Region of probe measurement relative to the RPS discharge channel. Image at left shows measurement grid approximately to scale with the RPS.

Double probe trace evaluation was automated. There are several ways to analyze double probe traces, and the hyperbolic tangent fit was used in this experiment[3]. When both probe tips are of the same area and the voltage between them is swept until ion current saturation is achieved, the I-V characteristic is a hyperbolic tangent curve[4]. The probe data were smoothed and a least-squares hyperbolic tangent fit was performed according to Equation 1:

$$I(V) = A \cdot \tanh[B \cdot (V - E)] + C \cdot x + D \qquad \text{Eq. 1}$$

where A is the ion saturation current and B is proportional to the inverse of the electron temperature. The other coefficients are required to perform the fit, but are not of physical significance. The electron temperature is given by Equation 2:

$$T_e = \frac{e}{2kB} \qquad \text{Eq. 2}$$

Following this calculation, the electron temperature and relevant physical constants related to the probe and gas are used to calculate n_e according to Equation 3.

$$n_e = \frac{i_+}{eA_p}\sqrt{\frac{m_i}{kT_e}} \qquad \text{Eq. 3}$$

E. Test Procedure

The first goal of this experiment was to determine the operating characteristics of the RPS. The procedure was to vary the voltage on the anode from 100 V to 300 V in 50 V increments, then increase the magnet current to minimize the discharge current. This procedure was followed at three separate mass flow rates, with anode voltage, anode current, and magnet current recorded. A discussion of results can be found in the next section.

For the second part of this experiment the effects of anode mass flow rate, magnet current, and discharge current on plasma properties were explored using a double probe. The mass flow was held constant at 40 sccm while the discharge current and magnet current were varied in order to determine the effect of discharge current at constant magnet current and mass flow rate, as well as the effect of magnetic field with constant mass flow rate and discharge current. The discharge current and magnetic field were then held constant and mass flow rate was varied in order to examine the effect of mass flow rate on the discharge properties.

III. Results

A. RPS Operation

The operating characteristics of the RPS can be found in Table 1. The anode current reported is the minimum current possible as the magnet current was varied. Anode current vs. magnet current for each mass flow rate has the same trend for all cases. As magnet current is increased, the anode current decreases rapidly, and levels off for the 40 and 50 sccm cases (Figure 4). Further increases in magnet current caused the discharge to cease. Anode current vs. anode voltage was weakly affected by mass flow rate, as can be seen in Figure 5.

Table 1. RPS operating characteristics. The 'x' symbols indicate conditions where the RPS would not sustain a steady discharge.

Anode Voltage (V)	Anode Current (A)	Magnet Current (mA)	Tank Pressure (Torr)
30 SCCM			
100	0.03	73	7.70E-06
150	0.31	165	7.70E-06
200	1.43	188	7.80E-06
250	2.79	186	7.80E-06
300	x	x	x
40 SCCM			
100	0.04	64	9.10E-06
150	0.56	373	9.10E-06
200	2.37	232	9.10E-06
250	3.22	271	9.20E-06
300	4.53	246	9.30E-06
50 SCCM			
100	0.07	146	1.00E-05
150	1.43	730	1.00E-05
200	2.37	1271	1.00E-05
250	3.98	276	1.00E-05
300	4.17	425	1.00E-05

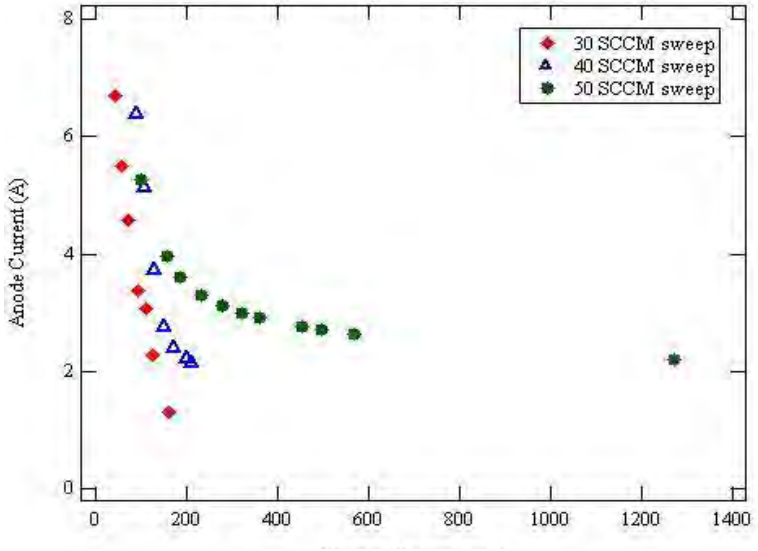

Figure 4. A comparison of anode current vs. magnet current for all flow rates.

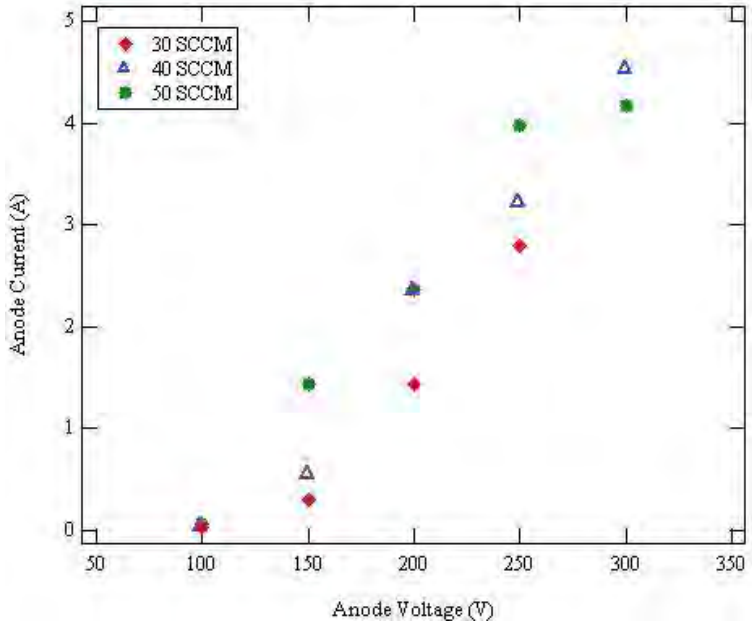

Figure 5. Effect of mass flow rate on anode I-V characteristic. Magnet current was adjusted at each anode voltage such that the anode current was minimized.

B. Probe Diagnostics

The probe data were analyzed and the effect of changing one of the three parameters (mass flow rate, discharge current, and magnet current) with the other two held constant was determined. For brevity, only one case will be presented for each of the three variables, however, the trends displayed apply to all measured conditions. Since the goal of the experiment was to determine whether the RPS plasma had density and temperature values that were available to the LTS technique, only those values are reported here.

1. Varying Mass Flow Rate, Constant Magnet and Discharge Current

For these comparisons the discharge current was held at 3 amps and the magnet current was fixed at 100 mA while the mass flow rate was varied. At 30 sccm the discharge voltage was 175 V and the pressure was 9.6 x 10^{-6} Torr, at 40 sccm the discharge voltage was 145 V and the pressure was 1.0 x 10^{-5} Torr, and at 50 sccm the discharge voltage was 99 V and the pressure was 1.2 x 10^{-5} Torr. As can be seen in Figure 6, there is minimal effect on the electron density as mass flow rate is changed. It is also apparent that the plasma produced by the RPS is asymmetric, though the reason for this phenomenon is unknown. The asymmetry is most likely caused by the position of the cathode, however other possibilities include asymmetric gas flow to the anode, asymmetric magnetic field, and slight variation in the alignment of the probe and RPS caused by heating of the aluminum mounting system during operation. As can be seen in Figure 7, as mass flow rate is increased electron temperature decreases, with the exception of an outlier that can be seen at the point farthest from the RPS on the centerline when the mass flow rate is 40 sccm.

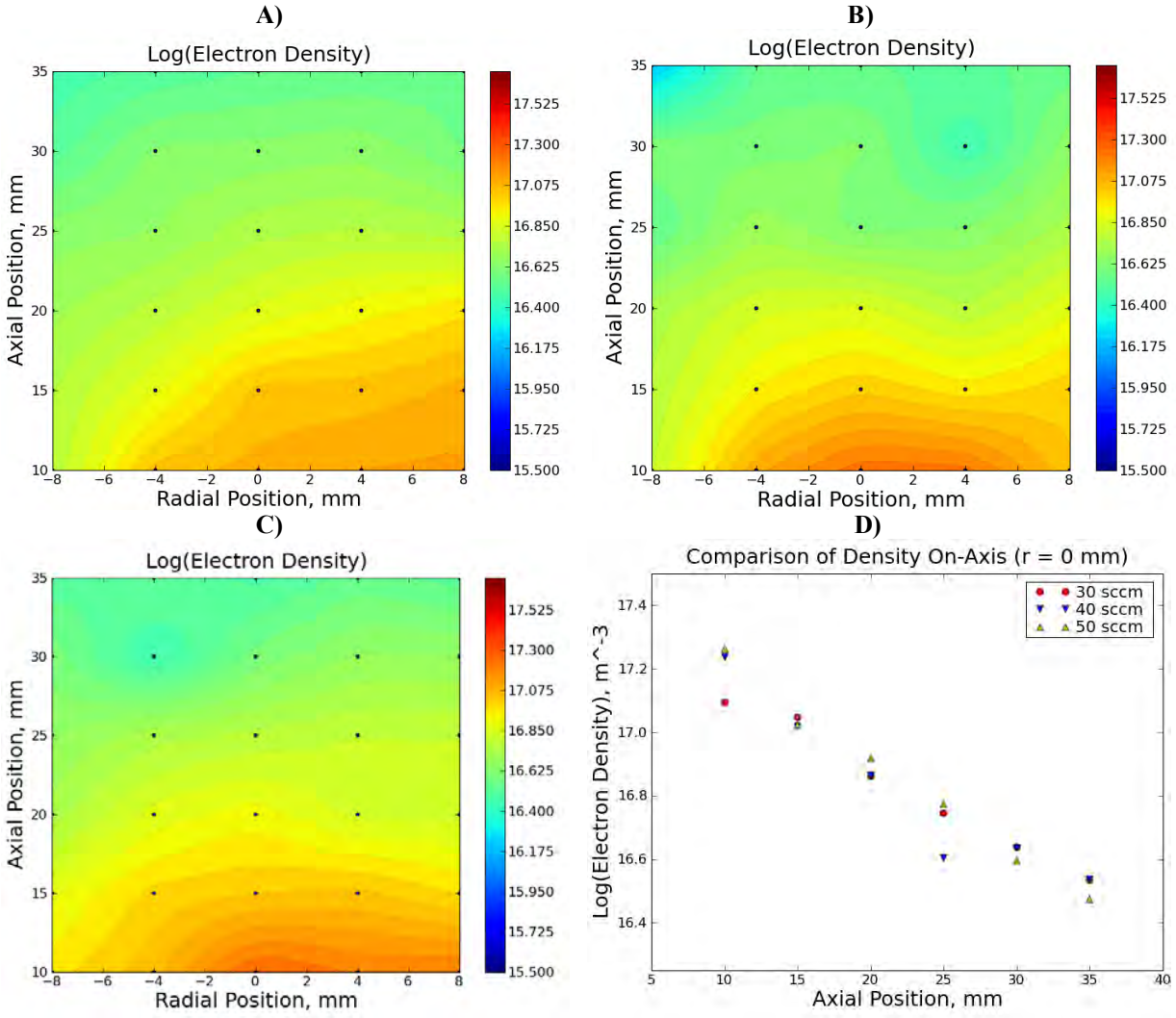

Figure 6. Logarithm of electron number density in m^{-3} at mass flow rates of A) 30 sccm, B) 40 sccm, C) 50 sccm, and D) a comparison of all three flow rates along the centerline.

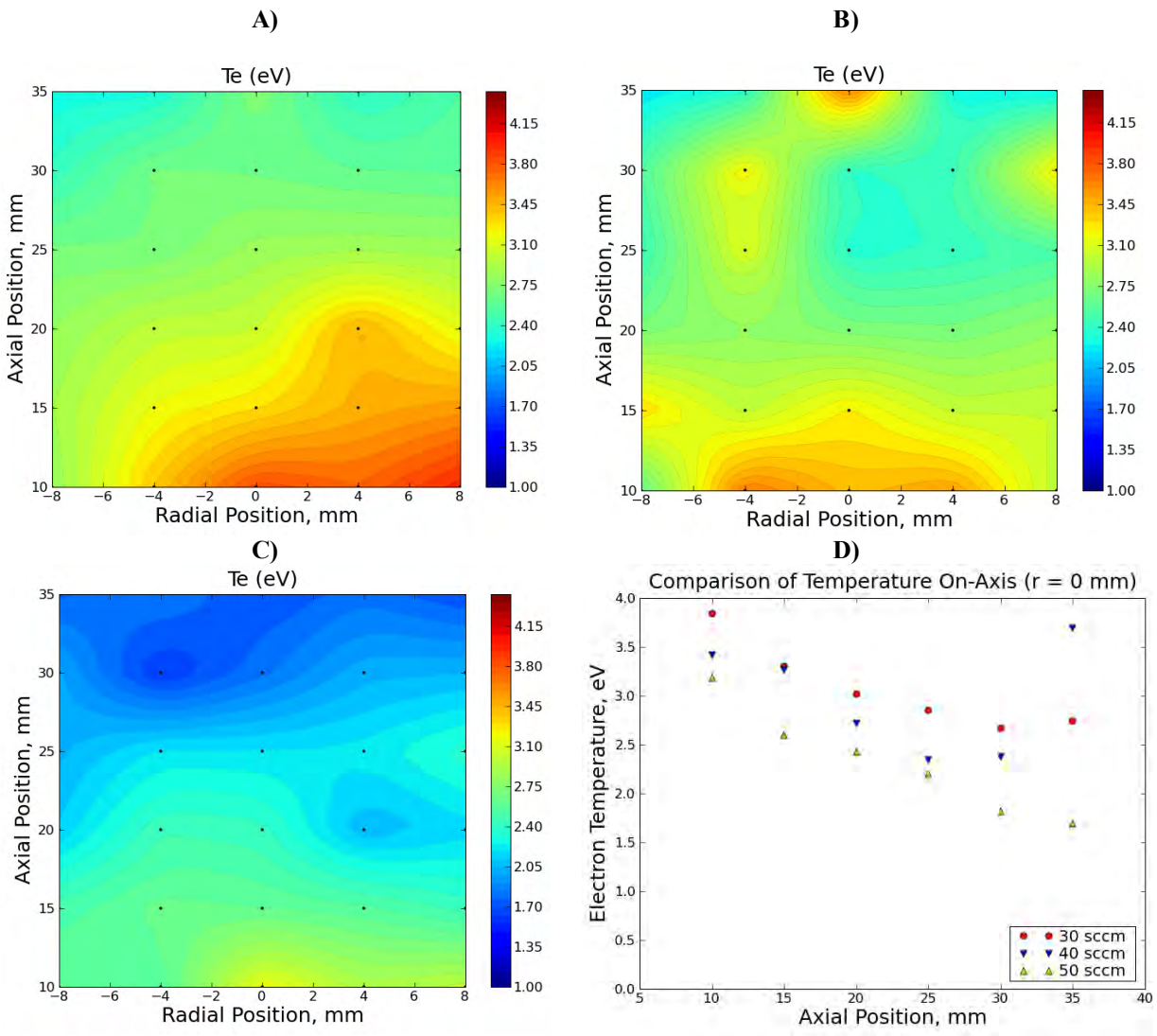

Figure 7. Electron temperature as measured at mass flow rates of A) 30 sccm, B) 40 sccm, C) 50 sccm, and D) a comparison of all three flow rates along the centerline.

2. Varying Discharge Current, Constant Mass Flow Rate and Magnet Current

For these comparisons the magnet current was held at 100 mA and the mass flow rate was fixed at 40 sccm while the discharge current was varied. When the discharge current was 1 A the discharge voltage was 109 V, at 2 A the discharge voltage was 117 V, and at 3 A the discharge voltage was 145 V. The pressure was 1.0 x 10^{-5} Torr for all discharge currents (due to constant mass flow rate). As can been seen in Figure 8, the number density of electrons increases as the discharge current is increased. As can be seen in Figure 9, there is minimal effect on the electron temperature as discharge current is changed. It appears that as discharge power is increased the energy is going into increasing the ionization fraction of the gas, and therefore the number density of electrons, instead of causing further heating of the electrons.

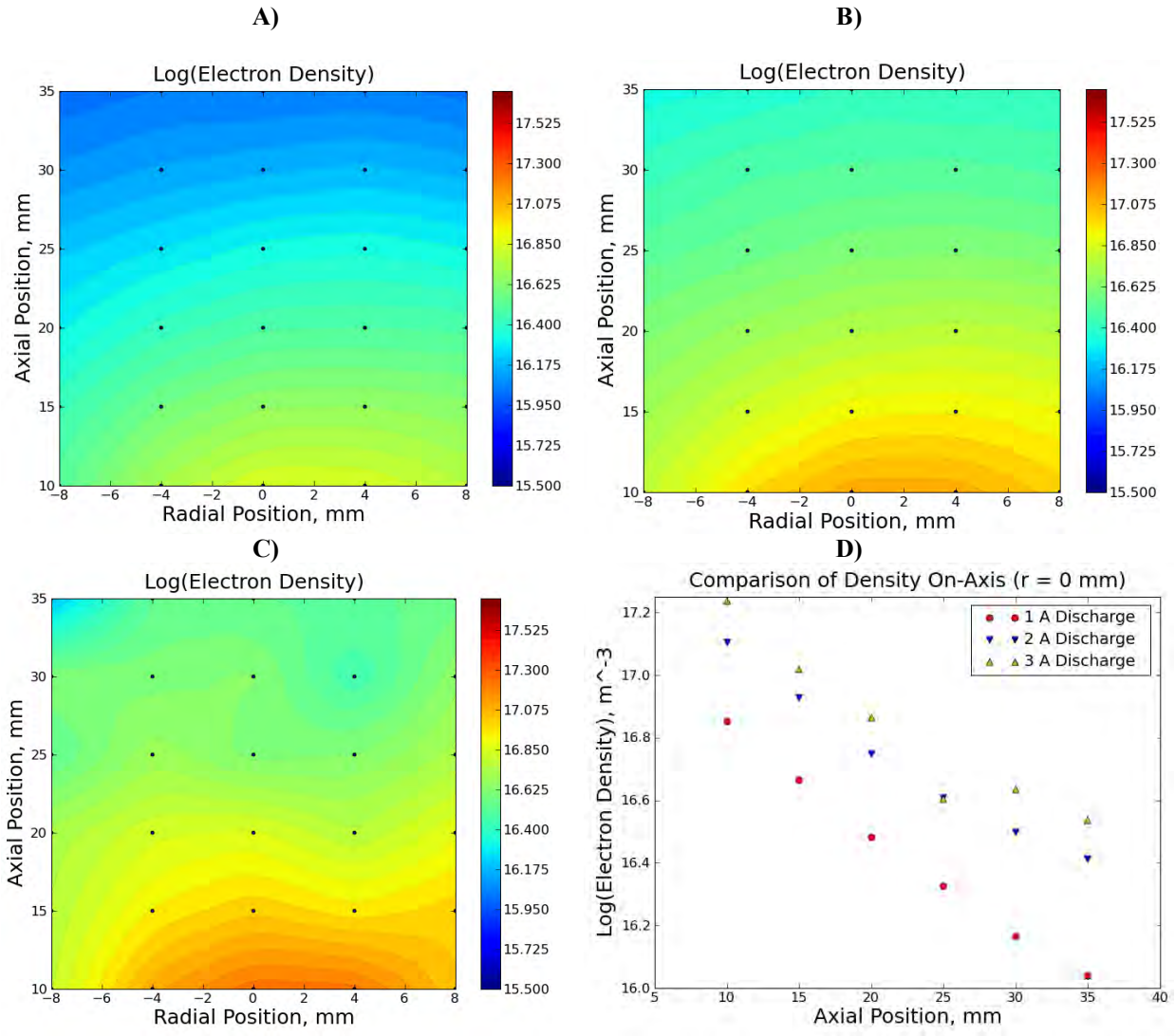

Figure 8. Logarithm of electron number density in m^{-3} at discharge currents of A) 1 A, B) 2 A, C) 3 A, and D) a comparison of all three discharge currents along the centerline.

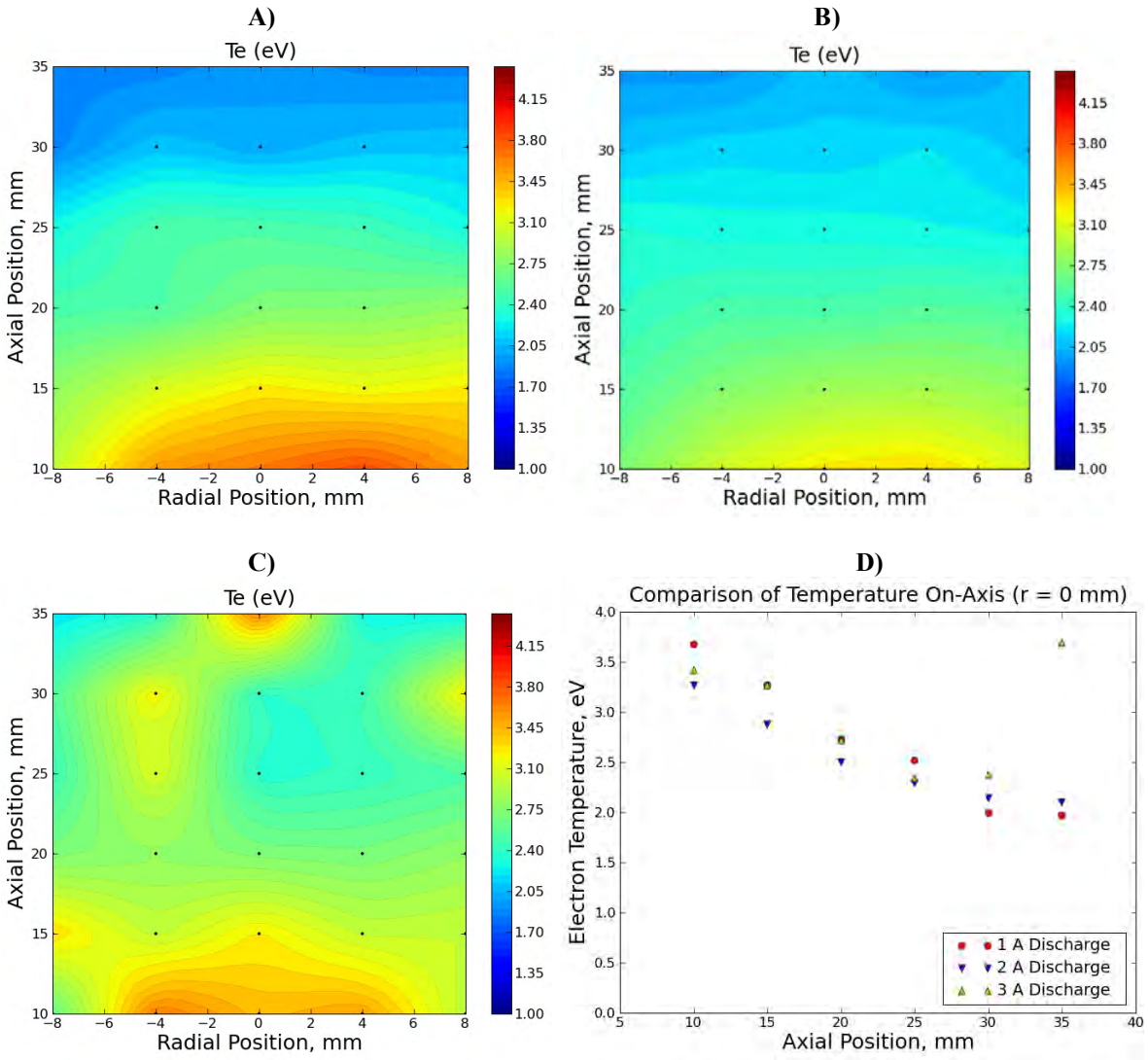

Figure 9. Electron temperature as measured at discharge currents of A) 1 A, B) 2 A, C) 3 A, and D) a comparison of all three discharge currents along the centerline.

3. Varying Magnet Current, Constant Mass Flow Rate and Discharge Current

For these comparisons the discharge current was held at 2 A and the mass flow rate was fixed at 40 sccm while the magnetic field was varied. When the magnet current was 50 mA the discharge voltage was 104 V, at 100 mA the discharge voltage was 117 V, and at 150 mA the discharge voltage was 143 V. The pressure was 1.0 x 10^{-5} Torr for all discharge currents . As seen in Figure 10, increasing magnet current caused an increase in electron density. Increasing the magnet current also caused an increase in electron temperature, as can be seen in Figure 11. While this trend was true for all measured cases, increasing the magnetic field above 150 mA caused the discharge to cease in all but one case during probe measurements (3 A discharge current, 50 sccm mass flow rate).

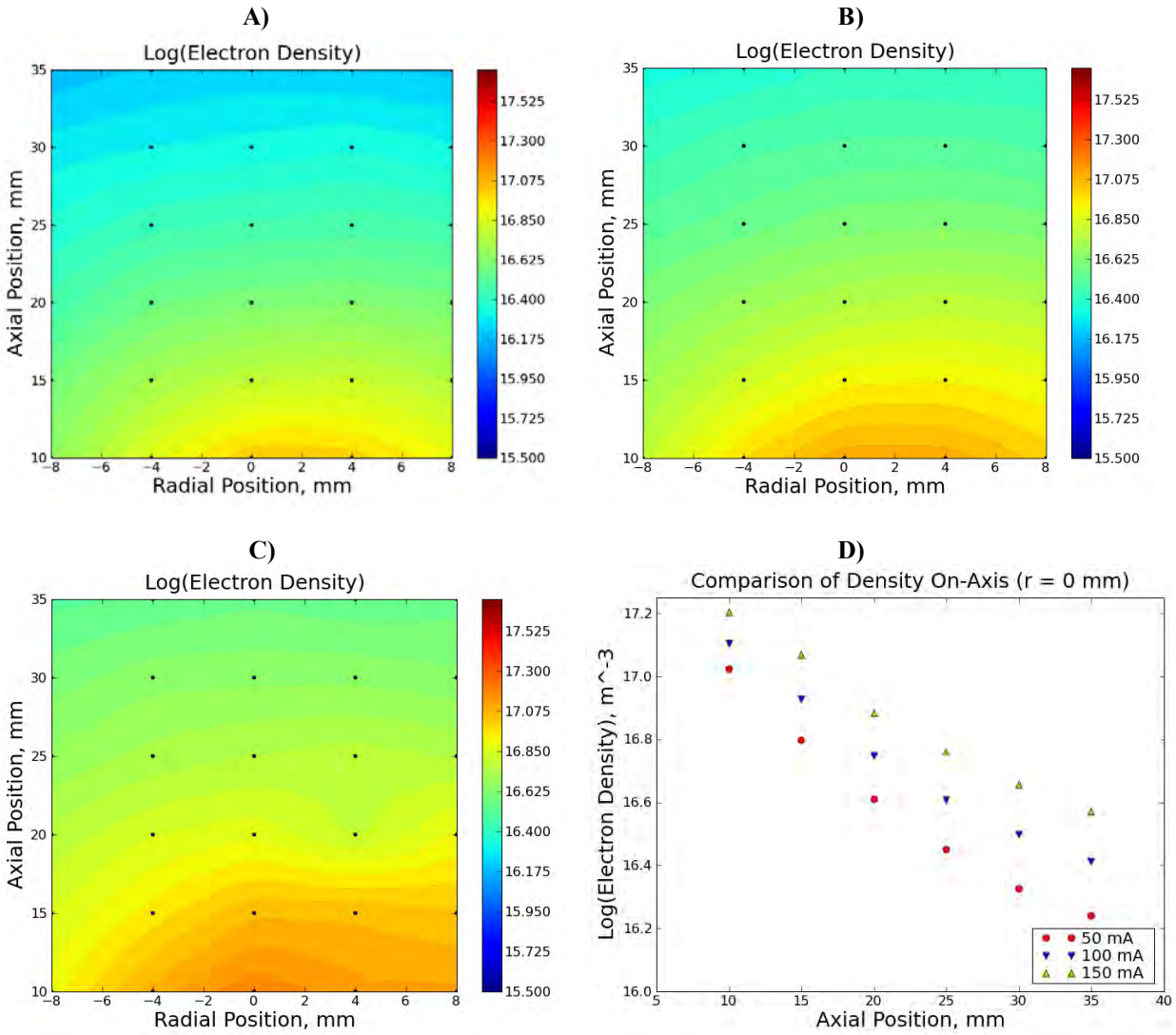

Figure 10. Logarithm of electron density in m^{-3} at magnet currents of A) 50 mA, B) 100 mA, C) 150 mA, and D) a comparison of all three magnet currents along the centerline.

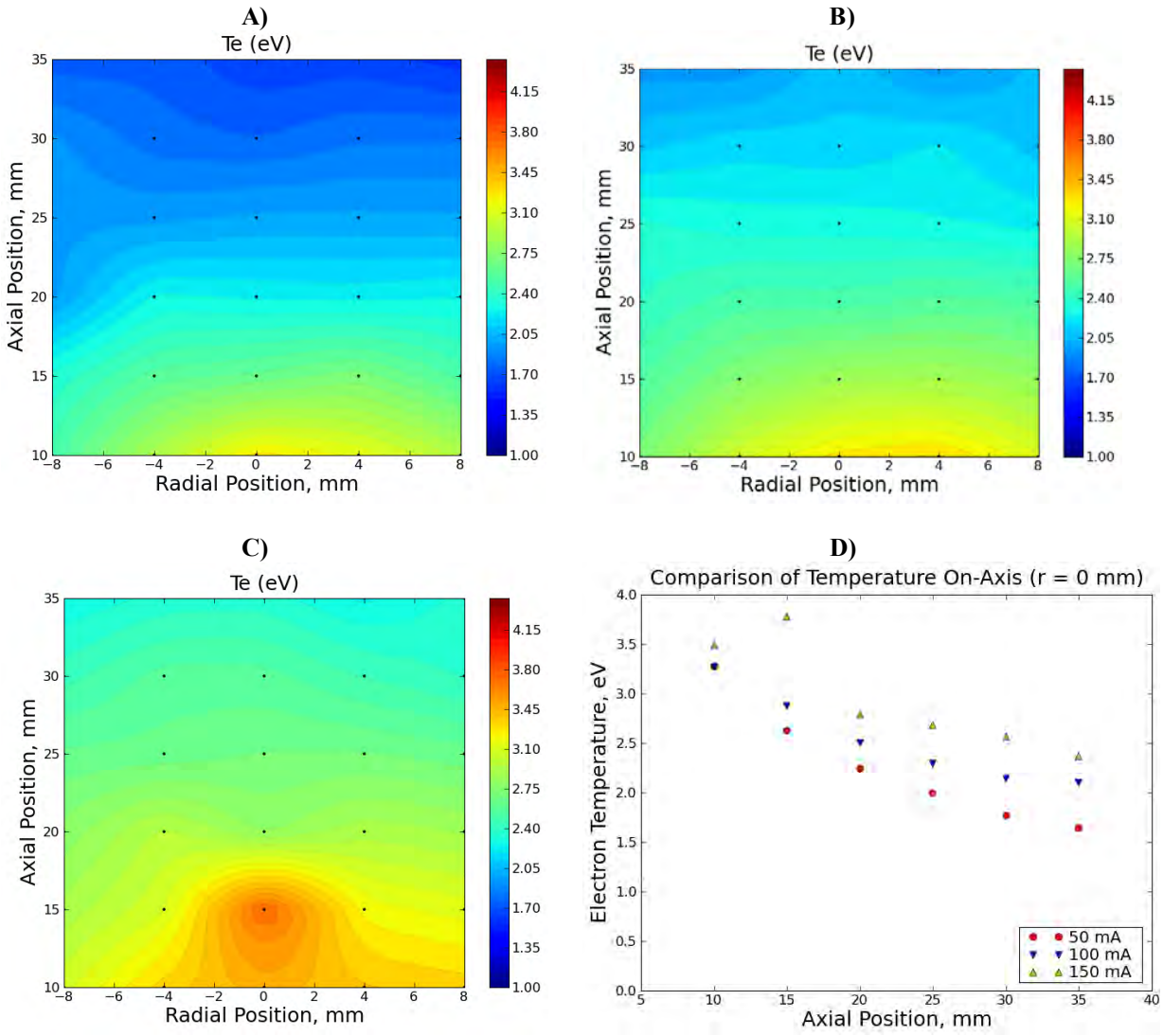

Figure 11. Electron temperature as measured at magnet currents of A) 50 mA, B) 100 mA, C) 150 mA, and D) a comparison of all three magnet currents along the centerline.

IV. Conclusions

The RPS was operated at a variety of conditions and the plasma near the channel exit was characterized using an electrostatic double probe. Electron temperature was found to range from 1 to 5 eV and electron density was found to range from 3 x 10^{15} m^{-3} to 6 x 10^{17} m^{-3}. These plasma conditions are similar to the results recently found by Sommerville[5], who measured the plasma properties in the near-field plume of a 2-kW HET. Sommerville reported average electron temperatures of approximately 4 eV and average densities of approximately 3.5 x 10^{17} m^{-3}, which indicates that the RPS plasma is a reasonable approximation to a HET plume and is suitable for use in validating the LTS technique prior to application on a HET.

In addition, the effects of mass flow rate, discharge current, and magnet current were determined. It was found that increasing the mass flow rate had no effect on electron density. Increasing the mass flow rate caused a decrease in electron temperature, presumably due to an increase in electron-neutral collisions. As discharge current was increased the electron temperature remained unchanged, while the density increased. It appears that the increase in discharge power went into increasing the fraction of ionized gas without affecting the electron temperature.

Increasing the magnet current caused an increase in both density and electron temperature. It is notable that the I-V characteristic of the RPS was not the same as a typical HET: as voltage was increased in the RPS the discharge current grew almost linearly. In a typical HET the discharge current is nearly constant over a large range of discharge voltages. It is possible that constant current behavior may be present at larger values of mass flow, however it was not observed between 20 and 50 sccm of krypton.

Acknowledgments

The first author would like to thank Jerry Ross for his assistance in motion-table control for this experiment.

References

[1] Muraoka, K., K. Uchino and M. Bowden, Plasma Phys. Control. Fusion 40, 1221 (1998).

[2] Van de Sande, M., "Laser scattering on low temperature plasmas" Ph.D. Dissertation, Eindhoven University of Technology, Eindhoven, Netherlands, 2002

[3] Washeleski, R.L. and King, L. B., "Characterization of the Plasma Plume from a LaB_6 Cathode: A Comparison in Probe Techniques". AIAA-2009-5199, *45th AIAA/ASME/SAE/ASEE Joint Propulsion Conference and Exhibit,* 2-5 August 2009, Denver, CO

[4] Huddlestone, R. H. and Leonard, S. L., *Plasma Diagnostic Techniques*, Academic Press, Inc., New York, 1965, Chap. 4.

[5] Sommerville, Jason D., "Hall-Effect Thruster--Cathode Coupling: The Effect of Cathode Position and Magnetic Field Topology", Doctoral Dissertation, Department of Mechanical Engineering-Engineering Mechanics, Michigan Technological University, 2009